

Automatic dimensionality reduction of Twin-in-the-Loop Observers

Giacomo Delcaro, Federico Dettù, Simone Formentin, *Senior member, IEEE*
and Sergio Matteo Savaresi, *Senior member, IEEE*

Abstract—State-of-the-art vehicle dynamics estimation techniques usually share one common drawback: each variable to estimate is computed with an independent, simplified filtering module. These modules run in parallel and need to be calibrated separately. To solve this issue, a unified Twin-in-the-Loop (TiL) Observer architecture has recently been proposed: the classical simplified control-oriented vehicle model in the estimators is replaced by a full-fledged vehicle simulator, or digital twin (DT). The states of the DT are corrected in real time with a linear time invariant output error law. Since the simulator is a black-box, no explicit analytical formulation is available, hence classical filter tuning techniques cannot be used. Due to this reason, Bayesian Optimization will be used to solve a data-driven optimization problem to tune the filter. Due to the complexity of the DT, the optimization problem is high-dimensional. This paper aims to find a procedure to tune the high-complexity observer by lowering its dimensionality. In particular, in this work we will analyze both a supervised and an unsupervised learning approach. The strategies have been validated for speed and yaw-rate estimation on real-world data.

Index Terms—vehicle dynamics, observer design, bayesian optimization, twin-in-the-loop, dimensionality reduction.

I. INTRODUCTION

A. Background

SINCE the 80s, car manufacturers and their tier-one vendors have been developing vehicle dynamics controllers that require unmeasured signals. In light of both physical and economic limitations, the measurement of these signals is impractical; thus, it becomes necessary to develop observers that estimate the missing variables. A thorough review on the topic is presented in [1]: in Table 1 the authors compare 33 state-of-the-art filters, which share one common drawback: they are only able to estimate a subset of states, such as tire forces, tire slip angles, vehicle sideslip and/or vehicle lateral velocity, etc. The adopted models are quite simple, *e.g.* single-track model to describe the lateral dynamic or quarter-car model for the vertical one. Due to the lack of one unified full-state filter, many observers are executed in parallel (see Figure 1 in [2]), often running in dedicated ECUs.

In recent times, the computational power available onboard vehicles has increased to the point where we are able to run a multibody vehicle simulator in real-time¹. We can adopt this virtual vehicle inside state estimators and advanced control architectures, as in the recent works by Riva et al. [3] and

Dettù et al. [4]–[6] and Delcaro et al. [7]. Since the vehicle simulator (or Digital Twin DT) is adopted inside the observer or the control architecture, we will refer to these schemes as *Twin-in-the-Loop* (TiL) systems. In [3], [5], the authors have already proven that the TiL architecture is able to outperform existing benchmarks on experimental data.

B. Motivations

In this paper, we will consider the TiL observer scheme, which exploits the DT as the model of the system, and corrects the virtual vehicle’s states in real time in order to track the real car with the simulated one.

Key advantages of using such an architecture are:

- 1) carmakers already use vehicle simulators in order to prototype and develop the vehicle, hence they do not need to develop a different model;
- 2) all vehicle’s states and variables of interest can be estimated simultaneously with one single observer. This means that a single observer has to be tuned.

Due to the intrinsic complexity of the vehicles’ simulator, we have to consider the DT as a black-box model whose inputs are the driver’s commands.

This is not the first time a unified observer for the entire vehicle has been put forth: the authors in [8] and [9] propose observers based on full-state white-box vehicle models, corrected in a Kalman-filter-like fashion. Despite being more accurate than the canonical single-dynamic observers, these filters still lack the fidelity of the simulation-based environment: the DT can easily deal with complex phenomena such as aerodynamic and floor effects, which play a fundamental role for both traction and stability when dealing with high-performing vehicles at high speeds.

The white-box approach is alternative to the TiL one, and poses other challenges, such as the tuning of the state and output covariance matrices, which have hundreds of entries. As analyzed in [3], [5] and [7] the main disadvantage of the TiL observer architecture is the black-box nature of the DT: there is no explicit analytical formulation of the model as a dynamic system. Therefore, we cannot adopt classical filter-tuning theory, such as (extended or unscented) Kalman filtering [10]–[12] or sliding-mode-observer tuning [13]. The correction matrix K can be tuned by solving a black-box optimization problem that aims at minimizing the difference between the real and the estimated states. In order to solve the optimization problem with statistical accuracy in spite of a small number of data samples, we will use Bayesian

The authors are with the Electronics, Computer Science and Bioengineering Department (Dipartimento di Elettronica, Informazione e Bioingegneria), Politecnico di Milano, Milan, Italy (email: giacomo.delcaro@polimi.it)

¹See, *e.g.*, <https://www.vi-grade.com/en/products/autohawk>.

optimization [14], discussed in section II-C. Matrix K relates the system outputs y to its states x (see Figure 1), hence it has $n_x \times n_y$ entries, where n_x is the number of states and n_y the number of outputs. Since we are dealing with the entire vehicle at once, n_x and n_y are in general large, and so is K . Optimizing a large number of parameters can be complex, due to this reason the authors in [3] select a-priori just 5 parameters out of the original 252 entries and focus on optimizing them, setting the remaining ones to 0.

The choice of the parameters to optimize can be suboptimal and represents one of the most critical aspects of the previous literature.

C. Related work

This paper focuses on introducing sparsity to an optimization problem. Bayesian optimization is very well known to be able to optimize only a handful of parameters, hence reducing the problem complexity significantly eases the optimization procedure. In [15]–[18], the authors state that BO is limited, in practice, at 10-20 optimization variables; in [19] the authors even limit its capabilities to 5-6 variables. In general, all black-box optimization algorithms suffer from the curse of dimensionality: in order to find convergence in large-scale black-box optimizations we need to have a lot of samples. One of the reasons behind this is that the higher the dimensions, the higher the average distance between samples: the expected distance between two random points in $[0, 1]^d$ approaches $\sqrt{d}/6$ [20]. Due to computational limits, the number of samples for our case study will be limited, and we will show that the optimization is far from convergence and overfitting. A typical way to decrease the optimization complexity lies in reducing the dimensionality of the problem. This can be realized by feature selection or feature extraction [21]. Feature extraction is usually more efficient than feature selection, since it does not discard the original features but finds a map from feature space into a new reduced subspace. Linear and non-linear methods for building the map exist. Examples of linear mapping [22] are Principal Component Analysis, Linear Discriminant Analysis, Factor Analysis; non-linear mappings [21] include kernel linear mapping, non-negative matrix factorization, manifold learning, etc.

Another approach for complexity reduction is the formulation of a sparse optimization (SO) problem. Sparse optimization [23] (SO) has been introduced in the last years in multiple fields: compressive sensing, image processing, matrix completion, and more in general information extraction. All the representations share the underlying rationale: minimizing the cardinality of one variable while satisfying some constraints. One of the milestones that made the development in this field possible is the 2006 theorem by Candès [24], which allowed to turn the NP-hard sparsity-imposing problem based on the ℓ_0 -norm into a convex problem that adopts the ℓ_1 -norm (under some Restricted Isometric Property or Uniform Uncertainty Principle).

One of the fields of research in SO is matrix completion [25], which aims at imposing sparsity to matrices by minimizing their rank (or, thanks to Candès' theorem, by

minimizing their nuclear norm [26]). While this theory may appear to align closely with our objectives, it's important to clarify that our primary aim is not to minimize the rank of the matrix but to alleviate the burden on the optimizer by focusing on reducing the cardinality of the matrices.

D. Main contributions

In the following, we will discuss two data-driven procedures to reduce the dimensionality of the optimization problem without introducing any prior to the system.

- 1) The first Dimensionality Reduction (DR) algorithm will be based on ℓ_1 -norm regularization and will be labeled *Supervised DR* (SDR). This data-driven technique consists of a two-stage optimization: the first black-box optimization sorts the optimization variables based on their impact on the estimator performance. The second stage of this algorithm is to optimize the sole performance of the filter, using the reduced set of variables.
- 2) The second DR algorithm has already been analyzed in one of our previous publications [7]. It is based on Principal Component Analysis (PCA) and is defined *Un-supervised DR* (UDR). In this work, a combined approach of SDR and UDR will be discussed.

All the results of the previously mentioned algorithms will be compared to a model-based DR (MBR).

We finally suggest a generic heuristic algorithm for dimensionality reduction.

E. Article structure

The paper is structured as follows. The problem statement is reported in Section II. Section III is devoted to building a Model-Based Reduction (MBR) benchmark. Section IV focuses on the Supervised Dimensionality Reduction (SDR) approach, and Section V covers the Unsupervised Dimensionality Reduction (UDR) approach, while also showing SDR and UDR can be combined. We conclude the paper with some final remarks in Section VI.

II. PROBLEM STATEMENT

A. TiL Architecture

In Figure 1 the architecture of the TiL observer is reported. The scheme resembles the classical observer schemes, such as Luenberger observers or Kalman filters: the difference $e_y = y(t) - \hat{y}(t)$ between the model outputs and the measured ones is turned into a state perturbation e_x via matrix K . In discrete time this becomes a two-step procedure:

- 1) prediction step, performed internally by the DT:

$$\begin{cases} \hat{x}^-(t) = f(\hat{x}(t-1), u(t)) \\ \hat{y}^-(t) = h(\hat{x}(t-1), u(t)) \end{cases} \quad (1)$$

being $\hat{x}(t)$ the estimated state, $u(t)$ the driver input and $y(t)$ the measured signal. $f(\cdot)$ and $h(\cdot)$ model the DT's behavior and are unknown to the user.

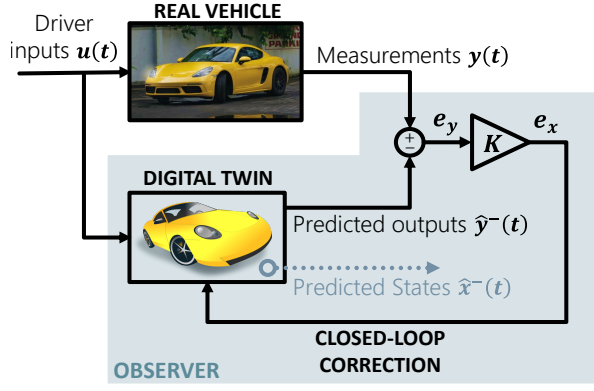


Fig. 1. Twin-in-the-Loop Observer architecture.

2) correction step:

$$\hat{x}(t) = \hat{x}^-(t) + K(y(t) - \hat{y}^-(t)) \quad (2)$$

In Figure 1, $e_x(t) = \hat{x}(t) - \hat{x}^-(t)$ and $e_y(t) = y(t) - \hat{y}^-(t)$. The sampling frequency of our sensors is 100 Hz , hence we will be correcting the DT every 10 ms .

Since the model of the system is highly non-linear, according to extended Kalman filters theory the correction law should be time-varying. In [3], the effectiveness of using just a *linear, time invariant* correction law has already been proven, hence we can adopt the same approach and optimize just one constant matrix K . The rationale behind this choice is the fact that the DT's outputs should be very close to the real ones, hence $e_y(t)$ will be very small, and the corrective term $e_x(t)$ will be small too (but necessary to track the real vehicle with the simulator). A time-varying matrix K would not considerably improve the results, but it would make the tuning problem much more complicated.

B. Performance optimization

Let us now define the procedure to tune matrix K in a data-driven fashion. The first step is to gather some data. In order to prove the capabilities of the TiL scheme, we will choose a scenario in which single-dynamic observers do not usually perform well: a high-performing vehicle in a racing circuit, where multiple dynamics are excited simultaneously. Moreover, the driver was asked to drive as aggressively as possible.

In the preliminary data acquisition, we need to measure both the vehicle's outputs $y_{meas}(t)$ and some states $x_{meas}(t)$. This is necessary since we will need to minimize the difference between the estimated states $\hat{x}(t)$ and the measured ones $x_{meas}(t)$. Note that the measurement of the states is only necessary in the initial phase to tune K and will not be required any further. In order to minimize the difference

between measured and estimated states, a generic loss function

L_K can be defined:

$$L_K(x_{meas}, \hat{x}) = \sum_{i=1}^{n_x} w_{x_i} rms(x_{meas_i} - \hat{x}_i) \quad (3)$$

$$\text{being: } rms(e_i) = \sqrt{\frac{1}{L} \sum_{l=1}^L e_i(l)^2}$$

w_{x_i} are the weights given to each state, which are used to both normalize the different magnitudes of the states and sort the states' importance. $e_i(l)$ is the l -th sample of signal e_i , which has L total samples.

Thus, we can minimize the estimation error by selecting K such that L_K is minimized. We can formulate this as an optimization problem:

$$K = \arg \min_K L_K(x_{meas}, \hat{x}) \quad (4a)$$

$$\text{s.t. } k_{i,j} \in [\underline{k}_{i,j}, \bar{k}_{i,j}] \quad \forall i = 1, \dots, n_x \quad \forall j = 1, \dots, n_y \quad (4b)$$

Being $k_{i,j}$ element (i, j) of matrix K . Equation (4b) is a constraint on the range of all entries of K . $\bar{k}_{i,j}$ and $\underline{k}_{i,j}$ are respectively the upper and lower bounds for the optimization variables $k_{i,j}$.

C. Parallel bayesian optimization

Let us now select the optimization algorithm to solve problem (4). The cost function depends on \hat{x} , which in turn depends on the black-box internal behavior. Therefore, we do not have any prior knowledge on L_K , which can in general be non-convex. Moreover, in order to evaluate the cost function on a selected matrix K , we must simulate the DT, which is computationally expensive. Due to these reasons, local optimizers or optimizers which require a large number of objective function evaluations cannot be used (see section 2.3 in [7]). One of the most efficient classes of global optimizers is the one based on surrogate functions [27]–[29]. This class of algorithms computes the next point to evaluate by minimizing an *acquisition function* $a(K)$, which finds a trade-off between exploring the unknown regions and exploiting the current knowledge of the position of the minimum. In order to estimate the unknown cost function $L(K)$, at each iteration i these optimizers use the previously $i - 1$ sampled points to build a *surrogate* or *meta* model $\hat{L}_i(K)$.

We will adopt one of the most used in this class of optimizers: the Bayesian Optimization (BO) algorithm [14]. BO assumes L_K as a realization of a *prior* Gaussian Process (GP) [30] with zero mean and $\kappa(K, K')$ covariance (or *kernel*): $L_K \sim \mathcal{GP}(0, \kappa(K, K'))$.

At iteration i , we know the previously $i - 1$ sampled points: $\mathcal{D}_{i-1} = (K_{1,\dots,i-1}, L_{K_{1,\dots,i-1}})$, hence we can condition the prior GP and get a *posterior* GP: $L_K | \mathcal{D}_{i-1} \sim \mathcal{GP}(m_{post}(K), \kappa_{post}(K, K'))$. $L_K | \mathcal{D}_{i-1}$ can be used as a meta-model of the unknown cost function L_K . This step is known as Gaussian Process Regression (GPR).

We will adopt one of the most frequently used kernel functions for GP regression: the Matérn 5/2 function [30].

$$\kappa(K_m, K_n) = \sigma_f^2 \left(1 + \sqrt{5}r + 5r^2/3 \right) e^{-\sqrt{5}r} \quad (5a)$$

Where r is the notion of distance between K_m and K_n . In particular, to optimize the distance in a high-dimensional optimization, we can use the Automatic Relevance Determination (ARD) version of Matérn function, introduced in [31]. In ARD, each dimension is weighted by the *characteristic length-scales* ℓ_1, \dots, ℓ_d :

$$r = \sqrt{(K_m^{vec} - K_n^{vec})^T M (K_m^{vec} - K_n^{vec})} \quad (5b)$$

where $M = \text{diag}([\ell_1, \dots, \ell_d])^{-2}$ is a diagonal matrix and K_*^{vec} represents the flattening of matrix K_* into an \mathbb{R}^d vector. The higher ℓ_i , the smaller the impact of the i -th dimension on the GP. Thus, we are able to remove irrelevant dimensions. ARD is also known as Sparse Bayesian Learning (SBL) and has been proven effective in several fields (see [32]).

As acquisition function, the expected improvement function [15] is chosen.

Since we aim at tuning an observer, we do not know a priori whether the chosen K_i at iteration i will be asymptotically stable or not. We can cope with this problem by adding a coupled constraint (as in [33]): a constraint that can be evaluated only by sampling the objective function. The constraint is modelled as an additional GP and considered in the acquisition function a_i , to avoid sampling points in known unstable regions (see equation (8) in [34]).

For the correct initialization, the optimization algorithm needs n_{seed} initial points to start computing the meta-model. The algorithm terminates when reaching a fixed number of iterations, defined as N .

As can be deduced from the preceding discussion, surrogate-function-based optimizers adopt a sequential optimization approach: we first need to sample a point, then build the surrogate model in order to determine the next point to evaluate. We can speed up this procedure using *parallel Bayesian optimization* [35]: we can use multiple parallel workers to sample different points simultaneously. When a worker is free, parallel BO assigns it a new point to evaluate by using all the previously sampled data enlarged with the points which are currently being sampled by other workers. In order to enlarge the dataset the algorithm requires an imputation method. We will use the *model-prediction* method (or *kriging believer* heuristic in [35]), which imputes the value of the objective function $L(K)$ as the mean of the GP at point K . Since we are dealing with high-dimensional models, which can make overly optimistic predictions, the imputed value is then saturated so as not to be smaller than the minimum sampled point so far. This method is known as *clipped-model-prediction*.

We can sum up parallel BO as in Algorithm 1.

D. Case study

To validate the observer's effectiveness, it is essential to thoroughly assess and challenge its capabilities through stress testing. For this reason, the driver was instructed to push the car to its limits, aiming to excite all vehicle dynamics concurrently. The data presented in this paper refers to a high-performing vehicle assessed on a racing track. In particular,

Algorithm 1: Pseudo-code for parallel BO

```

1: Select  $N$  number of total iterations,  $n_{seed}$  number of
   initial points ( $n_{seed} < N$ ) and  $P$  parallel workers
2: Sample  $n_{seed}$  seed points using all workers
3:  $i \leftarrow n_{seed} + 1$ 
4: while  $i \leq N$  do
5:   if at least one worker is free then
6:     If some workers are busy evaluating points,
       impute the values of  $L_K$  in those points
7:     Using the available (actual and imputed) data,
       build a GP model for the objective function
       and the constraints
8:     Compute the acquisition function  $a_i(K)$ 
9:      $K_i \leftarrow \arg \min_K a_i(K)$ 
10:    Evaluate  $L(K_i)$  on a free worker
11:     $i \leftarrow i + 1$ 
12:   end
13: end
14: Update the surrogate function
15: return best evaluated point and best predicted feasible
    point

```

two datasets will be used. The optimization dataset lasts 30 seconds and is reported in grey in Figure 2. The driving style is very aggressive, with sideslip angles higher than 23 degrees at more than 100 *km/h*. The validation dataset is quite aggressive too and consists of an entire lap of the track.

The available sensors onboard the vehicle are the following:

- 6-dof IMU (3D accelerometer and gyroscope) (6 signals);
- wheel encoders (4 signals).

Overall, there are 10 measured signals. In order to know the ground truth of our experiments, a Real-time-kinematic positioning system (RTK-GPS) was installed on the vehicle. Note that the GPS data will not be used as input to the observer, since it was mounted for testing purposes only. Besides, in typical driving scenarios GPS sensors suffer from availability and signal quality problems, caused for example by tall buildings or tunnels.

Due to the absence of suspension data, we will not deal with the vehicle's vertical dynamics. We will only make the DT track the real longitudinal and lateral dynamics. In order to do so, the cost function in (II-B) must weigh states which influence both dynamics. It is straightforward to verify that without one of the two, the DT will not be able to track the real vehicle. The chosen cost function is the following:

$$L_K(x_{meas}, \hat{x}) = \underbrace{rms(v_x - \hat{v}_x)}_{\text{long. dynamic}} + \underbrace{rms(\omega_z - \hat{\omega}_z)}_{\text{lat. dynamic}} \quad (6)$$

Where the yaw rate ω_z is expressed in *deg/s* while the longitudinal velocity v_x is in *km/h*. The first term in (6) is necessary to track the longitudinal dynamic of the real vehicle, while ω_z allows the DT to track the lateral movement of its real counterpart. Only one state per dynamic is used to keep the cost function as simple as possible.

VI-CarRealTime (CRT)² from VI-Grade will be used as off-the-shelf black-box vehicle simulator. CRT is commercially available and quite often used by car manufacturers for vehicle prototyping. To simulate the vehicle, CRT adopts 28 internal states:

- 3D position, orientation, linear and angular velocities;
- wheels' positions and velocities;
- suspensions' stroke lengths and velocities.

Since CRT can run on Simulink, we will use MATLAB function `bayesopt`³.

Correcting all 28 states with all 10 measured signals would generate a correction matrix with $n_x \times n_y = 280$ entries, which is far too highly dimensional for BO. Since running the digital twin is a computationally expensive task, we decided to limit the number of iterations to $N = 1000$. Imposing sparsity in the problem while maintaining the number of iterations can be beneficial: if the number of dimensions is too high the optimizer may not converge to the absolute minimum, while a reduced number of variables is more likely to converge to their absolute minimum. Nonetheless, it is to be noted that the absolute minimum for the original problem is better than (or, at least, exactly equal to) the reduced one, so the reduced problem may have a better convergence to an overall worse result.

In order to reduce the dimensionality of our case study, only a subset of states and outputs will be used in this paper. In particular, since no GPS data is available, we will not correct the vehicle's pose or its orientation. Since the front and rear wheels are highly coupled, only the velocity of one wheel for each pair will be corrected. As mentioned, no data from the suspensions is available, hence the vehicle's vertical dynamics will not be considered. For the same reason, roll and pitch rates and the vertical velocity will not be corrected. Finally, for the lateral dynamic we will only weigh ω_z , since it is directly measured and is involved in the cost function equation (6).

To sum up, we will only correct the following 4 states:

- v_x : longitudinal velocity
- ω_{fl} : FL wheel speed
- ω_z : yaw rate
- ω_{rr} : RR wheel speed

Finally, we need to select the outputs used to correct the aforementioned states. Since three of the four states are directly measured, we will use only the following outputs:

- ω_z : yaw rate
- ω_{rr} : RR wheel speed
- ω_{fl} : FL wheel speed

We are now dealing with a problem with cardinality $n_x \times n_y = 12$. Optimizing such a number of parameters with a surrogate-function-based optimizer probably will not converge to the best solution, but at least the problem is now manageable. We will now discuss how to tackle such a problem, and how reducing its dimensionality affects the performance, convergence, and computational times. The aim of this work does not reside in the pursuit of the best possible

observer or the estimation of the most complex dynamics, which was already proven in [3], but rather in formulating methodologies for the reduction of dimensionality of the filter.

III. BENCHMARK: MODEL-BASED REDUCTION

Before introducing the data-driven dimensionality reduction techniques (sections IV and V), we need to build a benchmark to compare the future results to.

Matrix K has 12 entries. Each element $k_{y_j \rightarrow x_i}$ indicates that state x_i is corrected using the error on the measurement y_j . We can leverage our prior knowledge of the system to eliminate certain optimization variables. For this reason, we will define this reduction Physics-Inspired Reduction or Model-Based Reduction (MBR). Furthermore, through parameter sorting, we can implement varying degrees of reduction, allowing us to investigate the impact of different reduction levels on the resultant outcomes. The most important parameters are the auto-correlated ones (i) (the ones in the lower diagonal of matrix K). The second and third class of parameters are respectively made of the parameters that relate the wheel speeds to the longitudinal velocity (ii) and cross-correlate the wheel speeds (iii). The last class relates lateral and longitudinal dynamics (iv).

- | | | |
|--|--|--|
| i) $k_{\omega_z \rightarrow \omega_z}$ | ii) $k_{\omega_{rr} \rightarrow v_x}$ | iv) $k_{\omega_z \rightarrow \omega_{fl}}$ |
| i) $k_{\omega_{fl} \rightarrow \omega_{fl}}$ | iii) $k_{\omega_{fl} \rightarrow \omega_{rr}}$ | iv) $k_{\omega_z \rightarrow \omega_{rr}}$ |
| i) $k_{\omega_{rr} \rightarrow \omega_{rr}}$ | iii) $k_{\omega_{rr} \rightarrow \omega_{fl}}$ | iv) $k_{\omega_{fl} \rightarrow \omega_z}$ |
| ii) $k_{\omega_{fl} \rightarrow v_x}$ | iv) $k_{\omega_z \rightarrow v_x}$ | iv) $k_{\omega_{rr} \rightarrow \omega_z}$ |

A. Optimization ranges heuristic

If we aim at solving equation (4), we need to know the optimization intervals for each variable (4b). Finding the range for the optimization variables can be one of the most difficult tasks for data-driven optimization algorithms. We will now briefly describe the rationale behind our choice of the ranges. The parameters will be split into three categories: auto-correlated ones (1) and cross-correlated wheels (2) and all the remaining ones (3).

- 1) Auto-correlated parameters: $k_{\omega_z \rightarrow \omega_z}$, $k_{\omega_{fl} \rightarrow \omega_{fl}}$ and $k_{\omega_{rr} \rightarrow \omega_{rr}}$. Since the dynamics of the system are quite slower than the DT update frequency (100 Hz), we can safely state that the states can be approximated as constants (they slowly change): $x_i(t+1) \approx x_i(t)$. If we plug this solution into the previously mentioned filter equations (1) and (2), we obtain: $\hat{x}_i(t+1) \approx \hat{x}_i(t) + k_{i \rightarrow i}(x_i(t+1) - \hat{x}_i(t))$, which is asymptotically stable if and only if: $k_{i \rightarrow i} \in (0, 2)$. In our tests, we have found that being close to 2 can lead to unstable filters. Thus, for safety reasons, we reduce the limit to $k_{i \rightarrow i} \in (0, 1.5)$.
- 2) Cross-correlated wheel parameters: $k_{\omega_{fl} \rightarrow \omega_{rr}}$ and $k_{\omega_{rr} \rightarrow \omega_{fl}}$. They are of the same nature of the previous $k_{\omega_{fl} \rightarrow \omega_{fl}}$, thus we will keep the span of 1.5 but center it in 0.
- 3) All remaining 7 parameters. The order of magnitude of the intervals is roughly given by $\text{range}(x_i)/\text{range}(y_j)$ ⁴.

²<https://www.vi-grade.com/en/products/vi-carrealttime/>

³<https://it.mathworks.com/help/stats/bayesopt.html>

⁴The range $x(t)$ is defined as: $\text{range}(x(t)) = \max_t(x(t)) - \min_t(x(t))$

C. Statistical analysis

In order to assess whether these properties statistically hold, each type of optimization must be repeated multiple times. We repeated each optimization 12 times. The solutions of the optimizations were all far from the variable range limits except for the 3-dimensional one, which sets all three auto-correlated parameters to their upper bound of 1.5.

The statistical results for the validation lap are reported in Figure 5. For each optimization type, 2 boxplots are depicted, one representing the *root-mean-square-error* of v_x and the other one the computational time taken by BO. The boxes represent the 25th and 75th percentiles of the distributions of the points, while the horizontal black line represents the median. The smaller dashed black lines illustrate the minimum and maximum recorded values. The cost $rmse(\omega_z)$ is not reported since ω_z is directly measured: it is weighted in the objective function to make the DT track the real system, but its performance of concern.

We can draw some conclusions on Figure 5:

- the loss function line (blue line in Figure 5) slightly decreases from 12 to 5 parameters, but it increases again for the 3-dimensional case. In the context of the original high-dimensional optimization problem (depicted on the left), achieving convergence to the optimal solution presents a challenge: only suboptimal solutions can be found. Conversely, excessively aggressive reduction (on the right), proves to be counterproductive due to the loss of critical degrees of freedom. The optimal balance, resulting in the best-performing solutions, is typically found between these two extremes;
- the variance tends to decrease as the dimensionality is reduced. This is due to the better convergence to the global minimum for the simplified problems;
- the computational time (orange line in 5) decreases with the number of parameters. An in depth analysis of this phenomenon is reported in section III-D.

In summary, pruning dimensions is beneficial in many ways: smaller computational effort, better convergence, better performance. The clear downside is that a too-aggressive reduction can lead to unsatisfactory performance.

D. Computational times

As shown in Figure 5, the computational times increase as the dimensionality of the process increases. At any iteration, BO first needs to estimate a GP meta-model of the objective function (step 7 in Algorithm 1), and later to minimize the acquisition function (step 9 in Algorithm 1).

Let us first analyze the computational times of building the surrogate model. GP regression has a complexity cubic with the number of input samples [36]: at iteration i fitting the GP has complexity $\mathcal{O}(i^3)$. If we sum all the computational times to build the GP at all iterations, we get an overall complexity of $\mathcal{O}(N^4)$, being N the number of BO iterations.

The covariance matrix of the GP depends on a kernel function, which depend on some notion of distance between samples [30]. Thus, the GP regression has a complexity that is linear

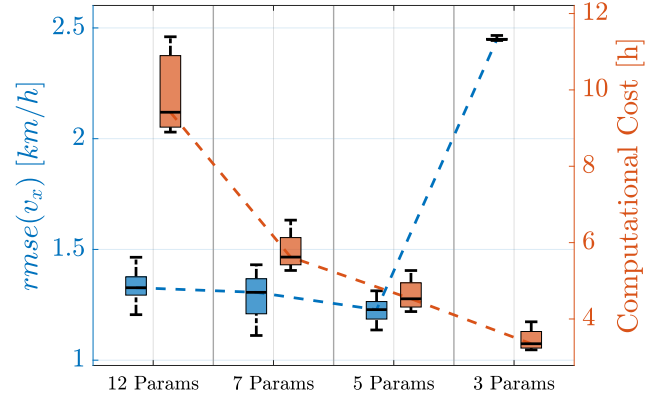


Fig. 5. MBR - Validation lap boxplot. Blue boxes report the distributions of the loss function for different degrees of reduction. Orange boxes represent the distribution of computational effort. The optimizations are ordered in decreasing order of optimization variables from left to right.

in the dimensions d : $\mathcal{O}(d)$.

Once the GP model has been computed, the acquisition function $a_i(K)$ must be minimized. Due to its non-convexity, the minimization process can be difficult and its complexity is largely determined by the adopted solver. In general, the computational effort is impacted by the dimensions d and by the complexity of the function to minimize.

To sum up, the increase in optimization time of Figure 5 is justified by the increases in complexity of both the GP regression step and the minimization of the acquisition function.

IV. SUPERVISED DIMENSIONALITY REDUCTION

In section III we have built the benchmark reduction (MBR) using apriori knowledge of the system. Our goal now is to find an automatic way of reducing the dimensionality of the problem from data. We will define this procedure as Supervised Dimensionality Reduction (SDR).

A. Sparsity requirement

In problem-solving, Sparse Optimization theory (SO) [23], [37] analyzes how the reduction of dimensionality can be beneficial for a problem. In particular, SO is used to find sparse solutions to undetermined linear systems. In our case, all the hypotheses that are typical of linear systems do not hold, but we can adopt the main ideas of sparse optimization. There exist three sparse problem formulations:

- ℓ_0 -constrained problem formulation:

$$K = \arg \min_K L_K(x_{meas}, \hat{x}) \quad s.t. \quad \|K\|_0 \leq T \quad (8a)$$

- function-constrained formulation:

$$K = \arg \min_K \|K\|_0 \quad s.t. \quad L_K(x_{meas}, \hat{x}) \leq \bar{L} \quad (8b)$$

- weighted formulation:

$$K = \arg \min_K L_K(x_{meas}, \hat{x}) + \lambda \|K\|_0 \quad (8c)$$

Where $\|K\|_0$ is the ℓ_0 norm of matrix K : $\|K\|_0 = \text{cardinality}\{k_{i,j} : k_{i,j} \neq 0\}$. T in equation (8a) is the

maximum allowed number of parameters different from 0 and \bar{L} in equation (8b) is a constraint on the maximum cost allowed. Finally, λ in equation (8c) is a hyperparameter of the optimization. According to the Lagrange multiplier theorem, a λ can be found such that problem (8c) is equivalent to (8a) or (8b).

The main issue behind equations (8) is the discontinuity given by the ℓ_0 norm: BO cannot correctly estimate highly discontinuous objective functions or constraints. In order to solve the problem we can adopt the same technique used in SO: we resort to ℓ_1 -norm minimization.

$$\|K\|_1 = \sum_{i,j} |k_{i,j}| \quad (9)$$

The most straightforward way of imposing sparsity to K would be to use formulation (8a) by adding the sparsity constraint to problem (7). Unfortunately, while it is easy to assign T for the ℓ_0 -norm constraint, it is difficult to choose it for the ℓ_1 norm. Adopting formulation (8c) can be challenging: the hyperparameter λ does not have physical meaning. In order to tune it, we could use cross-validation techniques, but this would require repeating many times a high-dimensional optimization, without any guarantee of convergence. Thus, we will use formulation (8b).

We can now formalize our sparse optimization problem, which aims at sorting the optimization variables by importance, exactly as we did in section III using our prior knowledge of the system. We will refer to this optimization as *Structure optimization*.

$$K = \arg \min_K \|\tilde{K}\|_1 \quad (10a)$$

$$s.t. \quad k_{i,j} \in [\underline{k}_{i,j}, \bar{k}_{i,j}] \quad \begin{array}{l} \forall i = 1, \dots, n_x \\ \forall j = 1, \dots, n_y \end{array} \quad (10b)$$

$$\mathcal{G}(K) \leq 0 \quad (10c)$$

$$rms(\omega_z - \hat{\omega}_z) < UB_{\omega_z} \quad (10d)$$

$$rms(v_x - \hat{v}_x) < UB_{v_x} \quad (10e)$$

In the objective function (10a), \tilde{K} contains all the normalized parameters $\tilde{k}_{i,j}$. Using the normalized parameters and not the original ones is crucial due to the varying orders of magnitude. The normalization is computed as follows:

$$\tilde{k}_{i,j} = \begin{cases} |k_{i,j} / \bar{k}_{i,j}|, & \text{if } k_{i,j} > 0 \\ |k_{i,j} / \underline{k}_{i,j}|, & \text{otherwise} \end{cases} \quad (11)$$

$$\forall i = 1, \dots, n_x, \quad j = 1, \dots, n_y$$

(by construction $\underline{k}_{i,j} \leq 0$ and $\bar{k}_{i,j} \geq 0$)

Constraint (10b) guarantees that the parameters are within the given optimization ranges and (10c) represents the set of K for which the filter is asymptotically stable.

Constraints (10d) and (10e) guarantee a satisfactory performance on both lateral (10d) and longitudinal (10e) dynamics. Thus, their role is to mimic the longitudinal and lateral dynamic terms in (7a). The Upper Bounds on the root-mean-square errors UB_{ω_z} and UB_{v_x} have physical meaning, hence they are much easier to select than the hyperparameter λ seen in formulation (8c). Differently from

Parameter	$\tilde{k}_{i,j}$	$k_{i,j}$	Parameter	$\tilde{k}_{i,j}$	$k_{i,j}$
$k_{\omega_{rr} \rightarrow \omega_{rr}}$	56.9%	0.85	$k_{\omega_{rr} \rightarrow \omega_{fl}}$	7.7%	0.058
$k_{\omega_z \rightarrow \omega_{rr}}$	55.6%	-0.83	$k_{\omega_{fl} \rightarrow \omega_{rr}}$	5.5%	-0.041
$k_{\omega_z \rightarrow \omega_z}$	42.2%	0.63	$k_{\omega_{rr} \rightarrow \omega_z}$	3.8%	0.0023
$k_{\omega_{fl} \rightarrow \omega_{fl}}$	41.5%	0.62	$k_{\omega_{fl} \rightarrow \omega_z}$	3.5%	-0.0021
$k_{\omega_z \rightarrow v_x}$	35.2%	0.53	$k_{\omega_{rr} \rightarrow v_x}$	2.1%	0.0095
$k_{\omega_{fl} \rightarrow v_x}$	26.2%	0.11	$k_{\omega_z \rightarrow \omega_{fl}}$	2.0%	0.030

TABLE II
RESULT OF THE STRUCTURE OPTIMIZATION (10).

(10b), these constraints share the same nature of (10c) and are unknown a priori.

In section III, the best optimizations had $rmse(v_x) \approx 1.1 \text{ km/h}$ and $rmse(\omega_z) \approx 0.6 \text{ deg/s}$. By setting $UB(v_x) = 1.5 \text{ km/h}$ and $UB(\omega_z) = 1.5 \text{ deg/s}$ we can still have very good performance for v_x and acceptable one for ω_z .

Note that we are now trying to solve a problem which seems to be more complicated than the original one (7): it has the same number of optimization variables but additional constraints. However, we are not seeking the true global optimum, but one feasible solution that tends to be the optimal one: if the performance constraints (10e) and (10d) are sufficiently strict, we are already guaranteed that the solution will be good enough. Once the solution of (10) has been found (or even a suboptimal solution), we know which are the most influential parameters for the optimization problem and we can run a lower dimensional optimization to only improve the performance (problem (7)).

Thanks to the structure optimization, we manage to turn a non-converging high dimensional performance problem (7) into a probably non-converging sparse optimization (10) followed by a reduced performance problem with a much greater probability of convergence to a better solution.

B. Structure optimization procedure

We are now able to run structure optimization (10), whose results are reported in Table II. In order to remove some of the optimization variables we need to select a threshold δ : all the optimal normalized $\tilde{k}_{i,j}$ which are smaller than δ will be pruned. Finally, the remaining parameters must be optimized according to the performance optimization problem (7).

In section III, we have selected varying degrees of reduction; to replicate the same effect three different thresholds δ are chosen: 0.05, 0.10 and 0.40. The resulting optimization classes will have 8, 6 and 4 parameters.

C. Statistical analysis

As in section III-C, to evaluate the statistical validity of these results we repeated 12 times each optimization class. The optimal K returned by each optimization was far from the variable range limits, with the only exception being the 4-dimensional case, where all three correlated parameters were set to their upper bound of 1.5.

The boxplots containing performance results for the validation

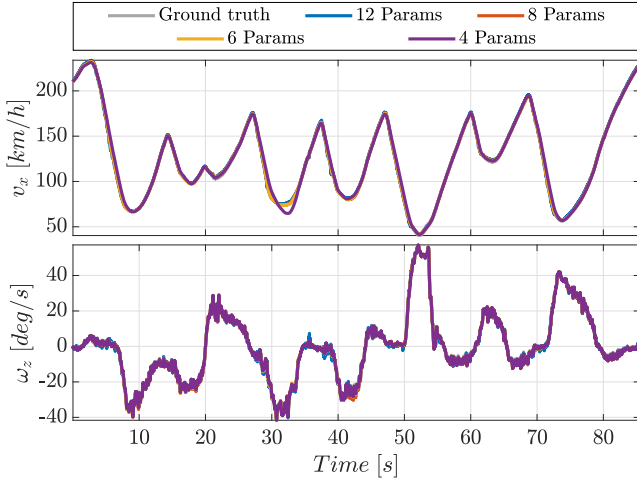


Fig. 6. SDR - Validation lap comparison. Filters with different numbers of parameters (colored lines) are compared against the ground truth (grey line).

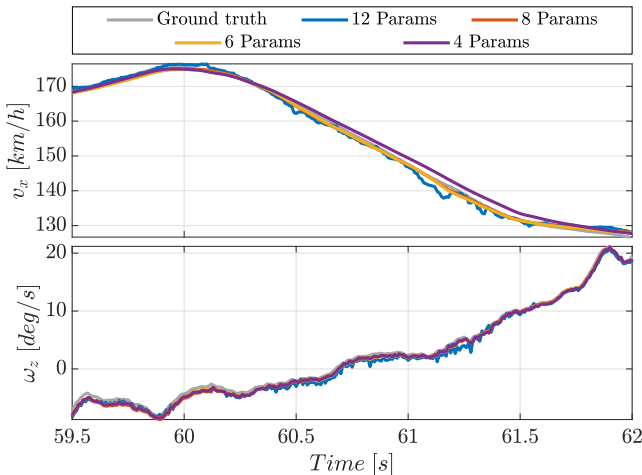


Fig. 7. SDR - Zoomed on Figure 6.

lap are reported in Figure 8. Optimizations are ordered from left to right in decreasing order of variables. We can draw similar conclusions to the MBR case (Figure 5):

- there is a clear parabolic trend in the average filter performance (blue dashed line): the high-dimensional optimization (on the left) is not converging to its global optimum, while the low-dimensional one (on the right) does not have all the degrees of freedom to converge to a well-performing solution;
- the variance in performance and computational times decrease with the number of parameters. The “+15h” label indicates the structure optimization time.

Overall, we can conclude that the dimensionality reduction is beneficial to improve the performance. The best solution (8-parameter one) is able to improve on average by 35% with respect to the original optimization. Note that this improvement comes with a computational cost: while the original optimization takes about 10 hours, the 8-dimensional one takes about $6 + 15 = 21$ hours! The lack of prior information results in increased computational overhead.

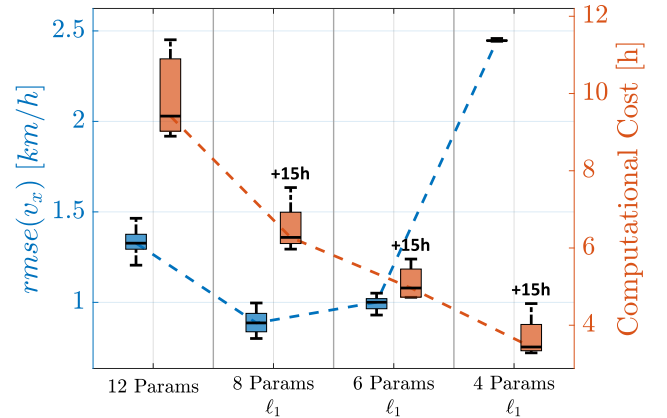


Fig. 8. SDR - Validation lap boxplot. Blue boxes report the distributions of the loss function for different degrees of reduction. Orange boxes represent the distribution of computational effort. The optimizations are ordered in decreasing order of optimization variables from left to right.

V. UNSUPERVISED DIMENSIONALITY REDUCTION

In this section, we will deal with numerically intractable problems. For the moment we have seen problems in which the solver is always able to find at least a “good enough” solution (as in the 12-dimensional case). If we considered correcting more states or using more system outputs, we would increase considerably the number of entries of K . This exact case is treated in our previous work [7]: 4 outputs and 4 states are considered, for a total of 16 optimization variables. We will now highlight the main contributions of [7] in order to be able to compare this method with the supervised method. The input space is now too highly-dimensional for BO: the problem is numerically intractable with our solver.

As mentioned in section I-C, we will now adopt a different way of imposing sparsity: we will use feature extraction to reduce the dimensions of the input to the observer (which are the system outputs). A visual representation of this is presented in Figure 9, where the TiL-Filtering scheme of Figure 1 is expanded with a feature-reducing map. The new correction matrix K_{red} has a number of inputs $\tilde{n}_y < n_y$.

In [7], the authors adopt Principal Component Analysis (PCA) to reduce the dimensionality of e_y from 4 to 3 dimensions, turning a 16-dimensional problem into a 12-dimensional one. Since the dimensionality reduction step is blind to the real performance objective, we will define this method Unsupervised Dimensionality Reduction (UDR).

The main issue which arises from the feature extraction step comes from the optimization variables upper and lower bounds (7b): they need to be specified in terms of K_{red} and not K . Theorem 1 in [7] finds a sufficient but not necessary condition that is able to turn the limits on K into limits on K_{red} as long as the feature extraction step is linear.

A. Statistical analysis

Since the optimization and validation datasets employed in [7] are the same as the ones adopted in this work, we will directly present the statistical analysis of the results. Refer

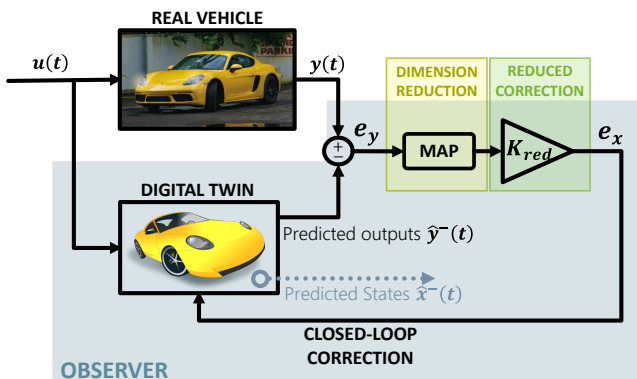


Fig. 9. Twin-in-the-Loop Observer architecture with input reduction.

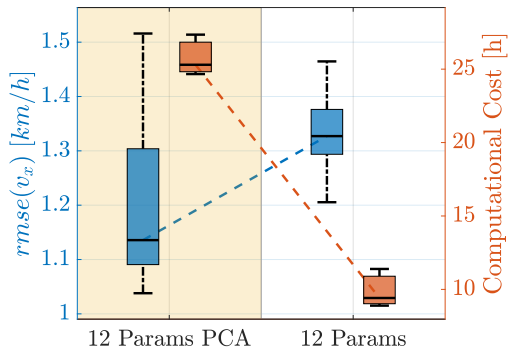


Fig. 10. UDR - Validation lap boxplot. Blue boxes report the distributions of the loss function for different degrees of reduction. Orange boxes represent the distribution of computational effort. The optimizations on the left are from the 16-dimensional case reduced to 12-dimensional using PCA; the ones on the right are the native 12-dimensional benchmark.

to [7] for any doubt in the methodology. Figure 10 reports the boxplots that compare the 16-dimensional optimization reduced to 12 using PCA and the native 12-dimensional benchmark.

Note that PCA is able to get better results on average (blue line), but at the cost of an increased variance and doubled computational effort. These drawbacks are not surprising: Theorem 1 [7] is only sufficient, hence the limits in K_{red} are intrinsically larger than their K counterpart. This introduces more complex unstable regions, which increase the number of unfeasible BO iterations, thus, the computational effort.

B. Combined SDR and UDR approach

Let us now study the combination of the previous supervised and unsupervised approaches.

In the previous section, we have analyzed a 12-dimensional problem reduced from a 16 one. We have stated multiple times that BO is not able to find the true optimal solution in such a high-dimensional space. Thus, let us apply SDR to our PCA-reduced solution. We will choose two values of δ : 0.07 and 0.1, which respectively correspond to removing 2 and 4 variables. More severe reductions (i.e. for $\delta > 0.1$) proved to be unstable. The validation laps for each optimization are reported in Figure 11.

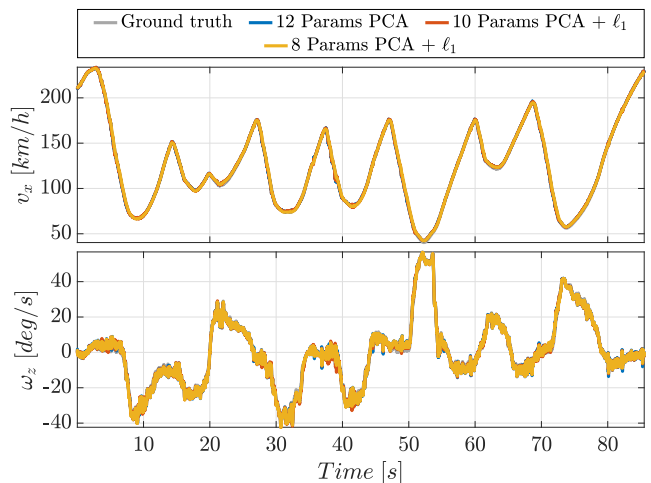


Fig. 11. Combined SDR and UDR approach - Validation lap comparison. Filters with different numbers of parameters (colored lines) are compared against the ground truth (grey line).

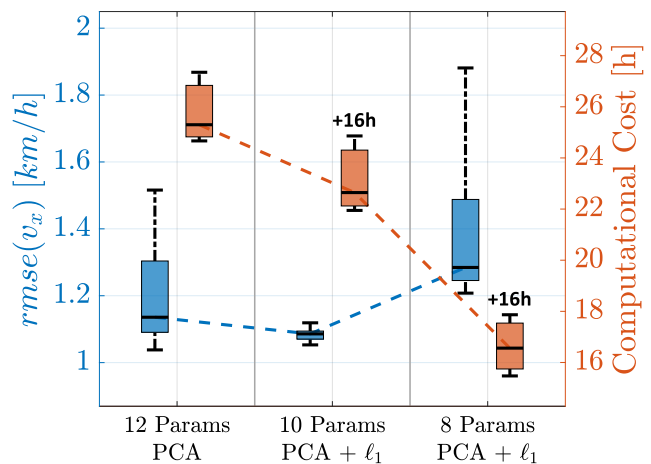


Fig. 12. Combined SDR and UDR approach - Validation lap boxplot. Blue boxes report the distributions of the loss function for different degrees of reduction. Orange boxes represent the distribution of computational effort. The optimizations are ordered in decreasing order of optimization variables from left to right.

The statistical results obtained by repeating each optimization type 12 times are reported in Figure 12. The parabolic trend present in 8 is also evident here. Due to the complexity of the feature extraction layer, the variance of the lower-dimensional case is not the smallest. This is even more evident if we remove more parameters, since the observer becomes unstable.

C. Overall comparison

Let us now compare the three techniques (MBR, SDR, and UDR). Figure 13 reports all the statistical analyses seen in Figures 5, 8 and 10 (Figure 12 is here not reported for the sake of simplicity). In the abscissae, the optimization types are ordered in decreasing number of optimization variables. Starting from the left, the first red column represents the native 16-dimensional problem reduced to 12-dimensional using PCA. The second column is the native 12-dimensional problem. The

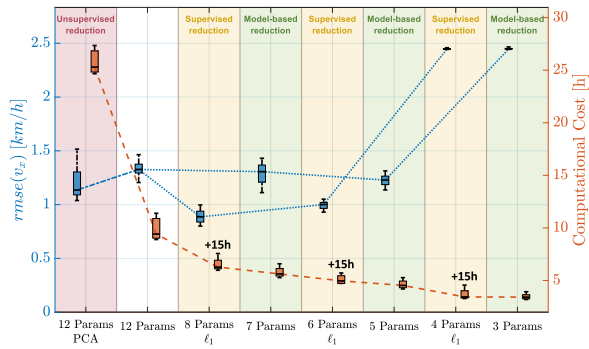


Fig. 13. Result comparison boxplot. This figure summarizes Figures 5, 8 and 10.

remaining 6 columns represent different reductions using MBR (green) and SDR (yellow). Note that the computational times (orange lines) are evidently decreasing with the complexity of the optimizations: this was studied in detail in section III-D. The computing effort for the unsupervised case is more than doubled with respect to all other optimizations, due to the additional complexity given by the PCA layer.

VI. FINAL REMARKS AND CONCLUSIONS

A. Heuristics for dimensionality reduction

Figure 14 represents a control flow diagram showing a heuristic on how to tackle problems as the one presented in the paper. When approaching a large-scale black-box optimization problem, we need to ask ourselves whether we can exploit any prior knowledge on the system. If the problem is not tractable – which is a vague definition, but we consider it to be so if the solver is not able to find a good solution in a reasonable time – we can only use UDR. Once the problem is again tractable, we can decide to reduce its dimensionality using SDR or directly run the performance optimization. The determination of which approach to take relies once again on the solver and the specific application and solver: it’s crucial to ascertain a deep knowledge of the number of variables that can be effectively optimized.

B. Conclusions

In this paper, we have studied two dimensionality reduction techniques for non-converging large-scale black-box optimization. In section III we have built a model-based benchmark (MBR), and in sections IV and V two different reduction approaches have been proposed: SDR and UDR. A combined approach of the two techniques has been analyzed in section V-B. All the reduction techniques have been tested on the performance optimization (Section 7) on a challenging scenario: a high-performing vehicle on a race track.

Thanks to the heuristic proposed in section III-A we were able to find all the parameters we needed to run optimization (7) with minimal prior knowledge on the system.

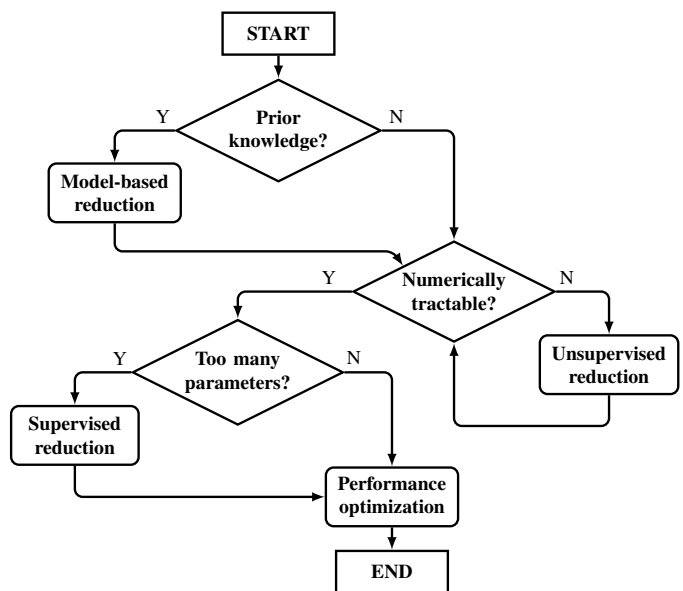


Fig. 14. Control flow diagram

ACKNOWLEDGMENTS

The authors are grateful to company VI-Grade GmbH for their technical support.

REFERENCES

- [1] K. B. Singh, M. A. Arat, and S. Taheri, “Literature review and fundamental approaches for vehicle and tire state estimation,” *Vehicle System Dynamics*, vol. 57, no. 11, pp. 1643–1665, 2019.
- [2] M. Viehweger, C. Vaseur, S. van Aalst, M. Acosta, E. Regolin, A. Alatorre, W. Desmet, F. Naets, V. Ivanov, A. Ferrara, and A. Vittorino, “Vehicle state and tyre force estimation: demonstrations and guidelines,” *Vehicle System Dynamics*, vol. 59, no. 5, pp. 675–702, 2021.
- [3] G. Riva, S. Formentin, M. Corno, and S. M. Savaresi, “Twin-in-the-loop state estimation for vehicle dynamics control: theory and experiments,” 2022. [Online]. Available: <https://arxiv.org/abs/2204.06259>
- [4] F. Dettù, S. Formentin, and S. M. Savaresi, “The twin-in-the-loop approach for vehicle dynamics control,” *IEEE/ASME Transactions on Mechatronics*, pp. 1–12, 2023.
- [5] F. Dettù, S. Formentin, and S. M. Savaresi, “Joint vehicle state and parameters estimation via twin-in-the-loop observers,” 2023. [Online]. Available: <https://arxiv.org/abs/2309.01461>
- [6] F. Dettù, S. Formentin, and S. M. Savaresi, “Robust tuning of twin-in-the-loop vehicle dynamics controls via randomized optimization,” in *Proc. 22nd IFAC World Congress*, 2023.
- [7] G. Delcaro, F. Dettù, S. Formentin, and S. M. Savaresi, “Dealing with the curse of dimensionality in twin-in-the-loop observer design,” in *Proc. 22nd IFAC World Congress*, 2023.
- [8] A. J. Rodríguez, E. Sanjurjo, R. Pastorino, and M. Ángel Naya, “State, parameter and input observers based on multibody models and kalman filters for vehicle dynamics,” *Mechanical Systems and Signal Processing*, vol. 155, p. 107544, 2021.
- [9] L.-Y. Hsu and T.-L. Chen, “Vehicle full-state estimation and prediction system using state observers,” *IEEE Transactions on Vehicular Technology*, vol. 58, no. 6, pp. 2651–2662, 2009.
- [10] R. E. Kalman, “A New Approach to Linear Filtering and Prediction Problems,” *Journal of Basic Engineering*, vol. 82, no. 1, pp. 35–45, 1960.
- [11] M. I. Ribeiro, “Kalman and extended kalman filters: Concept, derivation and properties,” *Institute for Systems and Robotics*, vol. 43, no. 46, pp. 3736–3741, 2004.
- [12] E. Wan and R. Van Der Merwe, “The unscented kalman filter for non-linear estimation,” in *Proceedings of the IEEE 2000 Adaptive Systems for Signal Processing, Communications, and Control Symposium (Cat. No.00EX373)*, 2000, pp. 153–158.
- [13] S. K. Spurgeon, “Sliding mode observers: a survey,” *International Journal of Systems Science*, vol. 39, no. 8, pp. 751–764, 2008.

- [14] B. Shahriari, K. Swersky, Z. Wang, R. P. Adams, and N. de Freitas, "Taking the human out of the loop: A review of bayesian optimization," *Proceedings of the IEEE*, vol. 104, no. 1, pp. 148–175, 2016.
- [15] P. I. Frazier, "A tutorial on bayesian optimization," 2018. [Online]. Available: <https://arxiv.org/abs/1807.02811>
- [16] D. Eriksson and M. Jankowiak, "High-dimensional Bayesian optimization with sparse axis-aligned subspaces," in *Proceedings of the Thirty-Seventh Conference on Uncertainty in Artificial Intelligence*, ser. Proceedings of Machine Learning Research, C. de Campos and M. H. Maathuis, Eds., vol. 161. PMLR, 27–30 Jul 2021, pp. 493–503. [Online]. Available: <https://proceedings.mlr.press/v161/eriksson21a.html>
- [17] R. Moriconi, M. P. Deisenroth, and K. Sesh Kumar, "High-dimensional bayesian optimization using low-dimensional feature spaces," *Machin Learning*, vol. 109, pp. 1925–1943, 2020.
- [18] M. Binois and N. Wycoff, "A survey on high-dimensional gaussian process modeling with application to bayesian optimization," *ACM Transactions on Evolutionary Learning and Optimization*, vol. 2, no. 2, pp. 1–26, 2022.
- [19] L. Sabug, F. Ruiz, and L. Fagiano, "SMGO- Δ : Balancing caution and reward in global optimization with black-box constraints," *Information Sciences*, vol. 605, pp. 15–42, 2022. [Online]. Available: <https://www.sciencedirect.com/science/article/pii/S0020025522004376>
- [20] M. Köppen, "The curse of dimensionality," in *5th online world conference on soft computing in industrial applications (WSC5)*, vol. 1, 2000, pp. 4–8.
- [21] W. Jia, M. Sun, J. Lian, and S. Hou, "Feature dimensionality reduction: a review," *Complex & Intelligent Systems*, vol. 8, no. 3, pp. 2663–2693, 2022.
- [22] J. P. Cunningham and Z. Ghahramani, "Linear dimensionality reduction: Survey, insights, and generalizations," *The Journal of Machine Learning Research*, vol. 16, no. 1, pp. 2859–2900, 2015.
- [23] S. Wright, "Sparse optimization methods," in *Conference on Advanced Methods and Perspectives in Nonlinear Optimization and Control*, 2010.
- [24] E. J. Candès, J. K. Romberg, and T. Tao, "Stable signal recovery from incomplete and inaccurate measurements," *Communications on Pure and Applied Mathematics*, vol. 59, no. 8, pp. 1207–1223, 2006.
- [25] E. Candès and B. Recht, "Exact matrix completion via convex optimization," *Commun. ACM*, vol. 55, no. 6, p. 111–119, jun 2012. [Online]. Available: <https://doi.org/10.1145/2184319.2184343>
- [26] E. J. Candès and Y. Plan, "Matrix completion with noise," *Proceedings of the IEEE*, vol. 98, no. 6, pp. 925–936, 2010.
- [27] N. V. Queipo, R. T. Haftka, W. Shyy, T. Goel, R. Vaidyanathan, and P. Kevin Tucker, "Surrogate-based analysis and optimization," *Progress in Aerospace Sciences*, vol. 41, no. 1, pp. 1–28, 2005.
- [28] A. I. Forrester and A. J. Keane, "Recent advances in surrogate-based optimization," *Progress in Aerospace Sciences*, vol. 45, no. 1, pp. 50–79, 2009.
- [29] A. Bemporad, "Global optimization via inverse distance weighting and radial basis functions," *Computational Optimization and Applications*, vol. 77, no. 2, pp. 571–595, 2020.
- [30] C. K. Williams and C. E. Rasmussen, *Gaussian processes for machine learning*. MIT press Cambridge, MA, 2006, vol. 2, no. 3.
- [31] D. J. MacKay and R. M. Neal, "Automatic relevance determination for neural networks," in *Technical Report in preparation*. Cambridge University, 1994.
- [32] S. H. Rudy and T. P. Sapsis, "Sparse methods for automatic relevance determination," *Physica D: Nonlinear Phenomena*, vol. 418, p. 132843, 2021. [Online]. Available: <https://www.sciencedirect.com/science/article/pii/S0167278921000014>
- [33] M. Khosravi, C. König, M. Maier, R. S. Smith, J. Lygeros, and A. Rupenyan, "Safety-aware cascade controller tuning using constrained bayesian optimization," *IEEE Transactions on Industrial Electronics*, vol. 70, no. 2, pp. 2128–2138, 2023.
- [34] M. A. Gelbart, J. Snoek, and R. P. Adams, "Bayesian optimization with unknown constraints," 2014.
- [35] D. Ginsbourger, R. Le Riche, and L. Carraro, "A multi-points criterion for deterministic parallel global optimization based on gaussian processes," 2008.
- [36] H. Liu, Y.-S. Ong, X. Shen, and J. Cai, "When gaussian process meets big data: A review of scalable gps," *IEEE Transactions on Neural Networks and Learning Systems*, vol. 31, no. 11, pp. 4405–4423, 2020.
- [37] Z. Zhang, Y. Xu, J. Yang, X. Li, and D. Zhang, "A survey of sparse representation: Algorithms and applications," *IEEE Access*, vol. 3, pp. 490–530, 2015.



Giacomo Delcaro received the B.Sc. and M.Sc. degrees (cum laude) in Automation and Control Engineering at Politecnico di Milano, Milan, Italy in 2020 and 2022, respectively. In September 2020, he joined the mOve Research Group as a M.Sc. student in the setting of the IndyAutonomousChallenge. In 2021, he spent four months in Indianapolis (USA) as software developer and vehicle engineer for the above-mentioned competition. In November 2022, he joined the mOve Research Group as a Ph.D. Student in Information Technology, Systems and Control area, at the Department of Electronics, Computer Sciences and Bioengineering (DEIB) of Politecnico di Milano. His research focuses on innovative data-driven estimation and control methods automotive systems.



control approaches for automotive systems.



Simone Formentin was born in Legnano, Italy, in 1984. He received the B.Sc. and M.Sc. degrees (cum laude) in automation and control engineering from Politecnico di Milano, Milan, Italy, in 2006 and 2008, respectively. He received the Ph.D. degree (cum laude) in information technology within a joint program between Politecnico di Milano and Johannes Kepler University of Linz, Linz, Austria, in 2012. After that, he held two postdoctoral appointments with the Swiss Federal Institute of Technology of Lausanne (EPFL), Lausanne, Switzerland and the University of Bergamo, Bergamo, Italy. Since 2014, he has been with Politecnico di Milano, first as an Assistant Professor, then as an Associate Professor. His research interests include system identification and data-driven control with a focus on automotive and financial applications. Dr. Formentin is the Chair of the IEEE Technical Committee on System Identification and Adaptive Control, the social media representative of the IFAC Technical Committee on Robust Control, and a Member of the IFAC Technical Committee on Modelling, Identification and Signal Processing. He is an Associate Editor for *Automatica* and the *European Journal of Control*.



Sergio Matteo Savaresi (Senior Member, IEEE) received the M.Sc. degree in electrical engineering from Politecnico di Milano, Milan, Italy, in 1992, and the M.Sc. degree in applied mathematics from Catholic University, Brescia, Italy, in 2000, and the Ph.D. degree in systems and control engineering from Politecnico di Milano, in 1996. After Ph.D., he was a Management Consultant with McKinsey & Company, Milan, Italy. Since 2006, he has been a Full Professor in automatic control at Politecnico di Milano, where he is Deputy Director and Chair of the Systems and Control Section of the Department of Electronics, Computer Sciences and Bioengineering (DEIB). He has been a Manager and Technical Leader of more than 400 research projects in cooperation with private companies. He is the Co-Founder of eight high-tech startup companies. He is the author of more than 500 scientific publications. His main research interests include vehicle control, automotive systems, data analysis and system identification, nonlinear control theory, and control publications, with a special focus on smart mobility.